Multiple conductances in the large K^+ channel from *Chara corallina* shown by a transient analysis method

S. D. Tyerman, B. R. Terry, and G. P. Findlay
School of Biological Sciences, The Flinders University of South Australia, Bedford Park, S.A. 5042, Australia

ABSTRACT The large conductance K^+ channel in the tonoplast of *Chara corallina* has subconductance states (substates). We describe a method that detects substates by monitoring the time derivative of channel current. Substates near to the full conductance tend to have long durations and high probabilities, while those of smaller amplitude occur with less probability and short duration. The substate pattern is similar in cell-attached, inside-out and outside-out patches over a range of temperatures. The pattern changes at high Ca^{2+} concentration (10 mol m^{-3}) on the cytoplasmic face of inside-out patches. One substate at ~50% of the full conductance is characterized by a high frequency of transitions from the full conductance level. This midstate conductance is not a constant proportion of the full conductance but changes as a function of membrane potential difference (p.d.) showing strong inward rectification. We suggest that the channel is a single pore that can change conformation and/or charge profile to give different conductances. The mean durations of the full conductance level and the midstate decrease as the membrane p.d. becomes more negative. Programs for analysis of channel kinetics based on an half-amplitude detection criterion are shown to be unsuitable for analysis of the K^+ channel.

INTRODUCTION

Patch-clamp techniques have shown that ionic channels in membranes can be viewed as pores that can change directly between conducting and nonconducting conformations. In the conducting conformation, channels may possess more than one level of conductance; for review, see Fox (1987). Channels which show multiple conductances include representatives from nearly all classes of channel yet found, even those formed by structurally simple synthetic peptides. The subconductance states (substates) generally occur with rather low probability and with short durations. However, dwell times at the substates and frequency of occurrence can be increased by various treatments including: aging of the preparation (Geletyuk and Kazachenko, 1985), excision of the membrane patch (Weik et al., 1989), application of blockers (Weik et al., 1989; Trautman, 1982; Kazachenko and Geletyuk, 1984; Lucchesi and Moczydlowski, 1990), use of different permeant ions and low pH (Pietrobon et al., 1988), use of different agonists (Auerbach and Sachs, 1984; Strecker and Jackson, 1989; Mistry and Hablitz, 1990), use of detergents (Sawyer et al., 1989), and low temperature (Hamill and Sakmann, 1981; Trautman, 1982; Patlak, 1989). Some ion channels can be modelled as multi-barrelled pores, usually on the basis that the main conductance is divided into obvious substates with equal portions of the main conductance (Miller, 1982; Hunter and Giebisch, 1987). These particular channels display long dwell times in the substates making analysis considerably easier and more reliable. Whether or not the long duration types with fully resolved substates are just extremes of the short duration type with unresolved substates remains to be seen (Lucchesi and Moczydlowski, 1990). Short duration substates can develop into long duration substates and vice versa (Geletyuk and Kazachenko, 1985; Weik et al., 1989). In this paper we describe experiments using low temperature, and different patch configurations in attempts to increase the dwell time and frequency of opening to substates.

The membrane surrounding cytoplasmic droplets isolated from the alga *Chara corallina* is thought to be tonoplast (Lühring, 1986). This membrane separates the vacuole and cytoplasm and plays a role in the regulation of solute concentrations in these compartments. A Cl^- channel and a large conductance K^+ channel which shows obvious substates have been characterized in the droplet membrane (Lühring, 1986; Tyerman and Findlay, 1989). At similar current amplitude the K^+ channels show qualitatively more open channel noise than Cl^- channels (Tyerman and Findlay, 1989). The extra noise of the open-state of the K^+ channel is almost certainly the result of many rapid transitions to other undetected levels. The *Chara corallina* K^+ channel has been modelled as a diffusion limited pore with fixed negative charge near the pore mouth (Laver and Walker, 1987; Laver et al., 1989). In such a model the current through the channel is limited by diffusion, while the pore diameter can be small enough to retain a high selectivity. However, the model does not account for the substates in the channel and equally does not provide an explana-

0006-3495/92/03/736/14 $2.00

tion for the high level of noise in the open state of this channel.

Analysis of multiple conductance levels requires a method that is not biased towards the single conductance state model of an ion channel such as the threshold crossing technique described by Sachs et al. (1982). More suitable methods identify conductance levels and events using criteria based on changes in variance (Patlak, 1989), transitions (Jackson, 1988), or transitions and thresholds (Vivaudou et al., 1986). A very sophisticated technique using signal processing techniques based on hidden Markov models has recently been published by Chung et al. (1990), but the procedure is not yet suitable for low probability substates where long records need to be processed.

A total amplitude histogram for a large data set contains information on the conductance levels of the channel and their individual open probabilities. However, two main sources of noise can swamp small peaks in the histogram. The first is thermal noise. The second is the inclusion in the histogram of points sampled from the record as a channel makes a transition from one level to another (the transition points). Finally, variation in amplitudes of principal conductance levels can cause large peaks to broaden and hide small adjacent peaks. We have developed computer software for detection of multiple conductance levels that is designed to: (*a*) select points from the data according to preset criteria of what constitutes a steady level of conductance, (*b*) average the amplitude at each level, and (*c*) remove the combined contributions of background noise and of transition points from the amplitude histogram. The software presents the activity of channels over time as a phase portrait in which the rate of change of current (dI/dt) is plotted against current (I). Such a phase portrait was used by Terry et al. (1991) to help characterize the substates and transitions in a complex anion channel from the plasma membrane of the plant *Amaranthus tricolor*. In a preliminary report we used these techniques to examine the K^+ channel in the cytoplasmic drop membrane of *Chara corallina* (Tyerman et al., 1989). Here we report in more detail on the technique and the several substates revealed in the *Chara* K^+ channel.

MATERIALS AND METHODS

Cytoplasmic droplets were collected from internodal cells of *Chara corallina* as previously described (Tyerman and Findlay, 1989). The droplets are probably bounded by the tonoplast membrane which surrounds the vacuole in vivo (Lühring, 1986). The vacuolar side of the membrane surrounding the droplets is exposed to the bathing medium. The bathing medium consists of a solution similar in ionic constituents to the vacuolar sap and compatible osmotically with it. The droplets were allowed to settle in the experimental chamber bathed in a standard solution consisting of (mol m^{-3}): 100 KCl, 10 CaCl2, 5 MES, 1.2 KOH, pH 5.5. Inside-out and outside-out patches were formed as described by Tyerman and Findlay (1989). The solutions bathing each membrane face will be indicated in the text when they differ from the standard bathing solution. Various treatments which may prolong or induce substates were examined. These were low temperature (down to 11°C, monitored with a thermistor placed near pipette), detergent, and patch excision in high and low calcium concentrations. Preliminary experiments with 2 μM Triton X 100 detergent (e.g., Sawyer et al., 1989) failed to reveal any obvious effect on substate occurrence and will not be discussed further.

The manufacture of pipettes, patch-clamp methodology, and recording systems were identical to those described in Tyerman and Findlay (1989). Recorded data was replayed and digitized (using ADCIN; Dr. J. Pumplin, Department of Physics, Michigan State University) after passing through a six-pole bessel filter. Unless indicated, segments of data were 30 s long and were sampled at 65 μs intervals with a filter cut-off of 2.74 kHz. The polarity of membrane potential differences (p.d.) and currents are indicated in the figure legends. In some cases these are given as pipette with respect to bath (more convenient for output from the software). For current/voltage curves the data have been corrected, including the resting membrane potential in drop-attached patches (see Tyerman and Findlay, 1989), to give the normal sign convention, i.e., cytoplasm with respect to vacuole.

Computer software for transition/amplitude (TRAMP) analysis of ion-channel recordings

Our method of detecting current levels in the digitized data relies initially on the detection of transitions. Transitions are detected by monitoring the rate of change of current (dI/dt) calculated from the amplitude difference between successive pairs of points divided by the time interval. When $|dI/dt|$ becomes larger than and crosses a preset threshold, a transition is flagged. The thresholds, positive and negative, for transitions are determined from a consideration of the noise and bandwidth (resolution) of the data. The thresholds must be of a level that prevents confusion between current changes caused by noise and those due to transitions, but should also be low enough to detect small transitions near to the limit determined by the bandwidth. Once a transition is registered, the new level is accepted for amplitude determination only if dI/dt remains between the thresholds (the analysis window) for a set period of time.

The basic principles of the analysis are illustrated in Fig. 1. Fig. 1 *a* shows I versus time for a theoretical square pulse of 10 pA amplitude and 0.5 ms duration through a Gaussian filter with a cut-off of 2.74 kHz. Fig. 1 *b* shows dI/dt versus I (rate-amplitude plot) for filtered pulses of 2 and 10 pA. The figure illustrates the parabolic trajectory of the transitions (positive and negative dI/dt) which is characteristic for a Gaussian filter and similar to the trajectory generated by a Bessel filter (Fig. 1 *d*). Fig. 1 *b* shows that the first points, measured as a transition enters the analysis window, are less than the actual amplitude of the recorded pulse. For any particular slope threshold, the proportion of the actual amplitude of a transition, reached as the analysis window is entered, depends on the magnitude of the transition. In this example, curves for transitions of 2 and 10 pA are shown. The dashed line represents a slope threshold of 10 pA/ms, and its intersection with the descending part of the curves gives the current level when the transitions reenter the analysis window. For the 2-pA transition, the intersect is at 85% of the level (1.75 pA), and for the 10 pA transition, the intersect is at 98% or 9.8 pA. A consequence of this is that the running average taken for a current while it remains within the analysis window will underestimate the magnitude of small and short transitions. This bias will become negligible the longer the

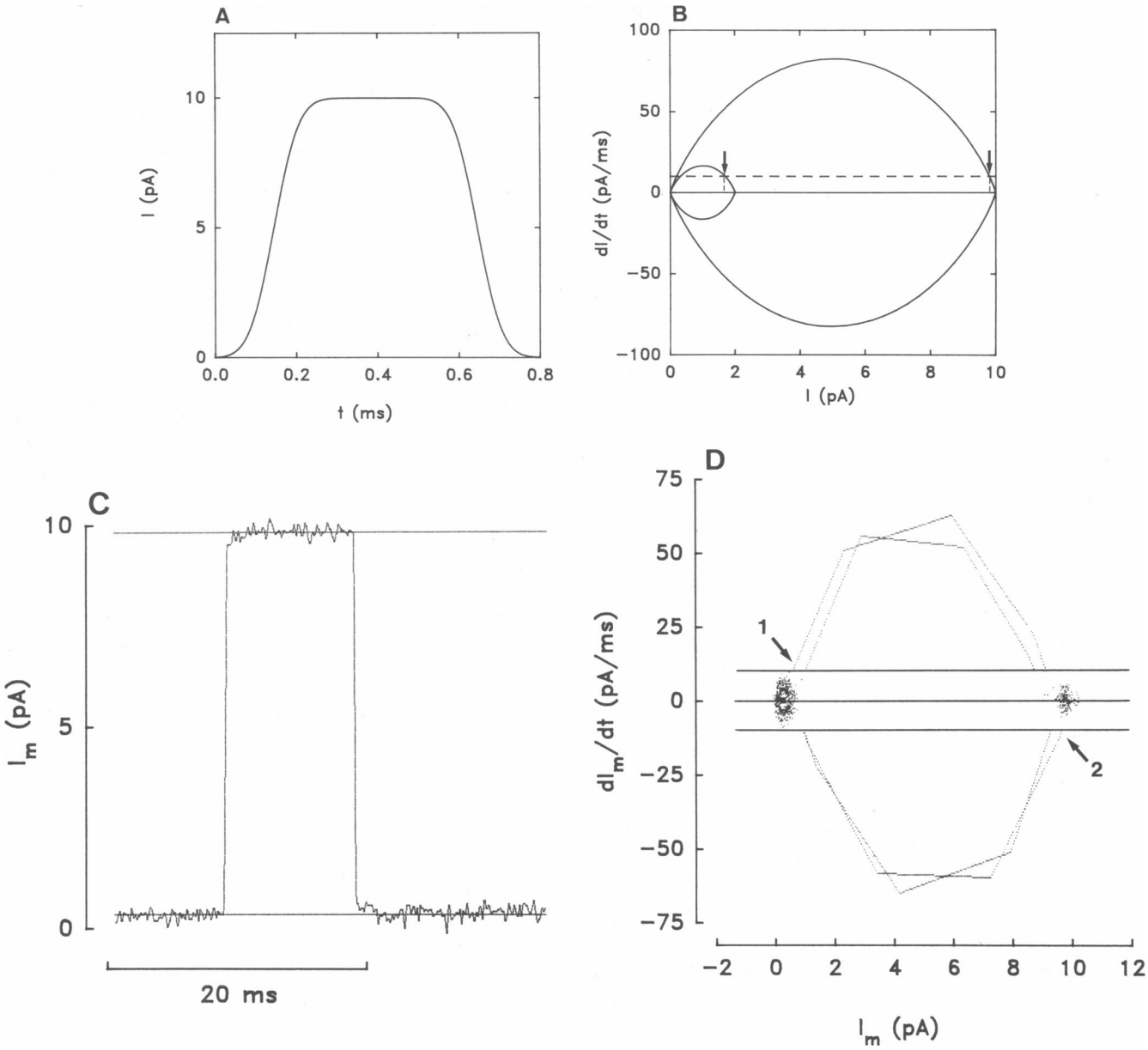

FIGURE 1 (*A*) Theoretical current versus time trace for a square pulse of duration 0.5 ms and amplitude 10 pA through a Gaussian filter with a cut-off (−3 db) of 2.74 kHz. (*B*) Rate (dI/dt) versus amplitude plot for the pulse shown in *A* and for a pulse 2 pA in amplitude. The dashed line is the upper slope threshold of 10 pA/ms. The arrows indicate the current amplitudes that are recorded when a positive transition reenters the threshold window. Curves were calculated using MathCAD V2.5 (Mathsoft Inc.) and the formulae given by Colquhoun and Sigworth (1983). (*C*) A 10-ms pulse recorded through the patch-clamp recording system with the same settings as for most of the experimental data. (*D*) The rate-amplitude plot for two 10-ms pulses and showing the slope thresholds (positive and negative) bracketing the noise on the steady current levels. The transition points are connected by lines in this case. The arrows marked 1 and 2 indicate where the duration count began and ended, respectively, for the open level.

current remains at a particular level. In practice we allow 10 sample intervals within the slope threshold before averaging is begun.

Since the maximum value of dI/dt (max) is proportional to the amplitude of a current transition for a given filter cut-off, small transitions will not be registered if their dI/dt (max) is less than the threshold dI/dt. In practice, the small transitions will appear as part of the noise because we set the dI/dt threshold near the maximum for the noise (Fig. 1 *d*). The minimum detectable transition for a particular threshold and filter cut-off can be determined from plots of the maximum value of dI/dt versus transition size. Efficient detection of transitions relies on obtaining the best estimate of dI/dt; thus, it is important to over-sample when digitizing the data. We used sampling

rates five times the cut-off frequency. The A/D recording resolution was better than 0.024 pA so that for data sampled at 65 μs intervals a dI/dt of the order of 0.3 pA/ms could be detected. This is small compared with the threshold of 10 pA/ms used to detect a transition, so that recording resolution is not a problem. A threshold dI/dt of 10 pA/ms will allow a theoretical minimum transition of ~1.2 pA to be detected.

A simulated channel event with noise, fed through the recording system, appears as shown in Fig. 1 *c*. The rate-amplitude plot generated by TRAMP in Fig. 1 *d* shows clusters of points at current levels (I_m) = 0 and 10 pA corresponding to the positions of the steady closed and open levels. The noise is bracketed by the thresholds in dI/dt. Straight lines connect the transition points outside this analysis window. In the other rate-amplitude plots with many points (Figs. 3 *a*, 6, 7, 9) lines between the transition points have been omitted for clarity. The duration of a particular current level is measured from the time that the trajectory crosses the slope threshold from a previous level to the time it next leaves the analysis window. These positions are indicated in Fig. 1 *d*. For a symmetrical pulse, i.e., one that returns to the level it started from, the method used here will give the correct duration, because the filter response is symmetrical for positive and negative transitions (Fig. 1 *b*). It is not clear, however, how the system will treat very short durations similar to the rise time for the filter (121 μs at 2.744 kHz), particularly because the sample intervals for the digitized data will be a large proportion of this. The durations recorded in the events list are those that satisfy the criteria that dI/dt remains within the analysis window for at least one sample point. It is important to consider possible sources of error in these recorded durations and to determine the minimum duration that may be reliably detected using the method. With short pulses, the durations measured will fluctuate depending on the position of the sample points with respect to the actual time course of the pulse. In some cases the pulse would be detected but no duration recorded because a value of dI/dt would not lie within the analysis window. Fig. 2 shows event durations, as would be measured by TRAMP, plotted against the actual duration of the test pulses. Noise was not included in the model used to derive the data in Fig. 2. For pulses less than 0.25 ms, more than 70% of the detected events have no duration measured and those that are measured are overestimated. It is possible for a very short event to a large amplitude to be recorded incorrectly as an event to a smaller amplitude; as an example, a pulse 0.05 ms in duration to 10 pA will only reach 3.95 pA through a 2.74 kHz filter. However, the program will miss more than 70% of such events for data recorded at 65 μs, and of the measured events all those less than 0.25 ms must be disregarded.

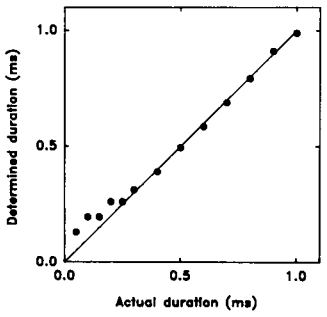

FIGURE 2 Measured durations using the detection criterion used by TRAMP as a function of actual durations. Durations were obtained using a MathCAD 2.5 routine in which the position in time of sample points varied randomly with respect to a Gaussian filtered pulse of variable duration. Filtering was 2.74 kHz and the sampling interval was 65 μs.

Software organization

The program makes a first pass through the recording of the raw data and computes the standard deviation (SD) of all successive values of dI/dt. A value of the standard deviation due to noise alone can be measured directly from a record in which no channels are active. The standard deviation is then used to set positive and negative thresholds of dI/dt. Thresholds of about $\pm 3 \times$ SD of dI/dt greatly reduce the chance that a noise peak will be mistaken for a transition between levels. A second pass through the recording compares dI/dt with the thresholds set from the first pass. While dI/dt remains between the thresholds the mean current for the event is calculated (running average), provided dI/dt has remained within the window for a predetermined length of time (normally 10 sampling intervals). The initial (10) sample points are included in the running average. When dI/dt goes outside the window the running average for I is terminated. The current value is followed as it transits between levels, until dI/dt reenters the window, and so on.

The program generates two types of amplitude histograms. The total amplitude histogram includes all points within the analysis window. Mean currents are used to construct a mean amplitude histogram where each mean is weighted by the duration of the event by multiplying the mean by the number of sample points in the event. This sharpens the amplitude histogram plot considerably. The difference between the total amplitude histogram and the mean amplitude histogram gives a rough measure of any rapid transitional activity in the channel, where dwell times are less than a defined interval. Mode currents are obtained from the mean amplitude distributions and are used as first estimates of the current amplitudes. These are calculated automatically and are shown for example in Fig. 4. All modes are included regardless of the number of events. Modes corresponding to small numbers of events will be less reliable as estimates of conductance levels, and this is taken into account in the initial estimation of substate levels.

To obtain durations from the events list a separate program is used which gathers the durations associated with a current range determined by the user. The range is set to cover the amplitude distribution for a particular current level. The distribution of durations is then analyzed using a MathCAD 2.5 procedure ignoring durations of <4 sample intervals. The events list is also used to generate a plot of amplitude versus duration and a frequency histogram of transitions.

The program also provides a plot of dI/dt versus current (I) (slope-amplitude plot) which gives a convenient summary of the whole record, because it shows the various amplitude levels as well as the positive and negative going transitions. A color or contour scale on the plot is used to depict different frequencies of events at each level of current. More information about the transitions can be obtained from examination of the trajectories of dI/dt vs. I during the transitions. The shape of the parabolic trajectory (generally) reflects the characteristics of the filter used on the raw data. Whether a transition is direct or occurs through a brief substate can be determined by comparing theoretical trajectories of square wave inputs of different amplitudes with the trajectories of actual channel transitions.

The software includes a median digital filter which was used on all the data shown in this paper. This removes some noise from the data without affecting the value of the maximum slope during a transition (i.e., it preserves edges) and requires little computational time. Further details of median filters can be obtained from Justusson (1981) and Tyan (1981).

Two other channel analysis programs were used to compare with the TRAMP analysis, IPROC and FETCHAN (Axon Instruments, Burlin-

game, CA). These employed detection of transitions based on the crossing of half the amplitude of the single channel current.

RESULTS

1. General characteristics

Characteristics of current flow through the K^+ channel in a drop-attached patch at 24°C are shown in Fig. 3. The rate amplitude plot for a large number of opening events clearly shows three nodes (clusters at $dI/dt = 0$) corresponding to the closed state and fully open state (mainstate), and a prominent substate halfway between (midstate). The parabolic clouds of points between the nodes show the transitions between the conductance states. Inspection of the rate amplitude plot reveals several other nodes between the main ones. These are determined by visual inspection of the amplitude frequency histograms (Fig. 3 *b*) and amplitude duration plot (Fig. 3 *c*). A more objective determination of these levels would need to take into account the number of events and the variation due to short durations in some cases. Inspection of the raw data can verify that the main levels are correctly placed (e.g., Fig. 4 *c*). Despite exclusion of transition points, the total amplitude histogram shows a long tail towards the closed level. This could signify that short closures have not been fully resolved or that there are many substates, only a few of which have lasted long enough to be resolved into the mean amplitude histogram.

Using criteria similar to those outlined by Fox (1987), it can be deduced that the various current levels actually represent substates of the channel rather than independently opening channels. The substates are not superpositions of channels passing currents in a different direction. If they were, the channels would be observed individually. A Cl^- channel, often active in drop-attached patches, together with the K^+ channel can give the appearance of a single channel with substates, particularly at pipette potentials between 0 and 50 mV. That the Cl^- channel cannot account for the substates is clear from the current-voltage curves for the midstate (see below) and from the fact that the general pattern of substate appearance is unchanged near the reversal

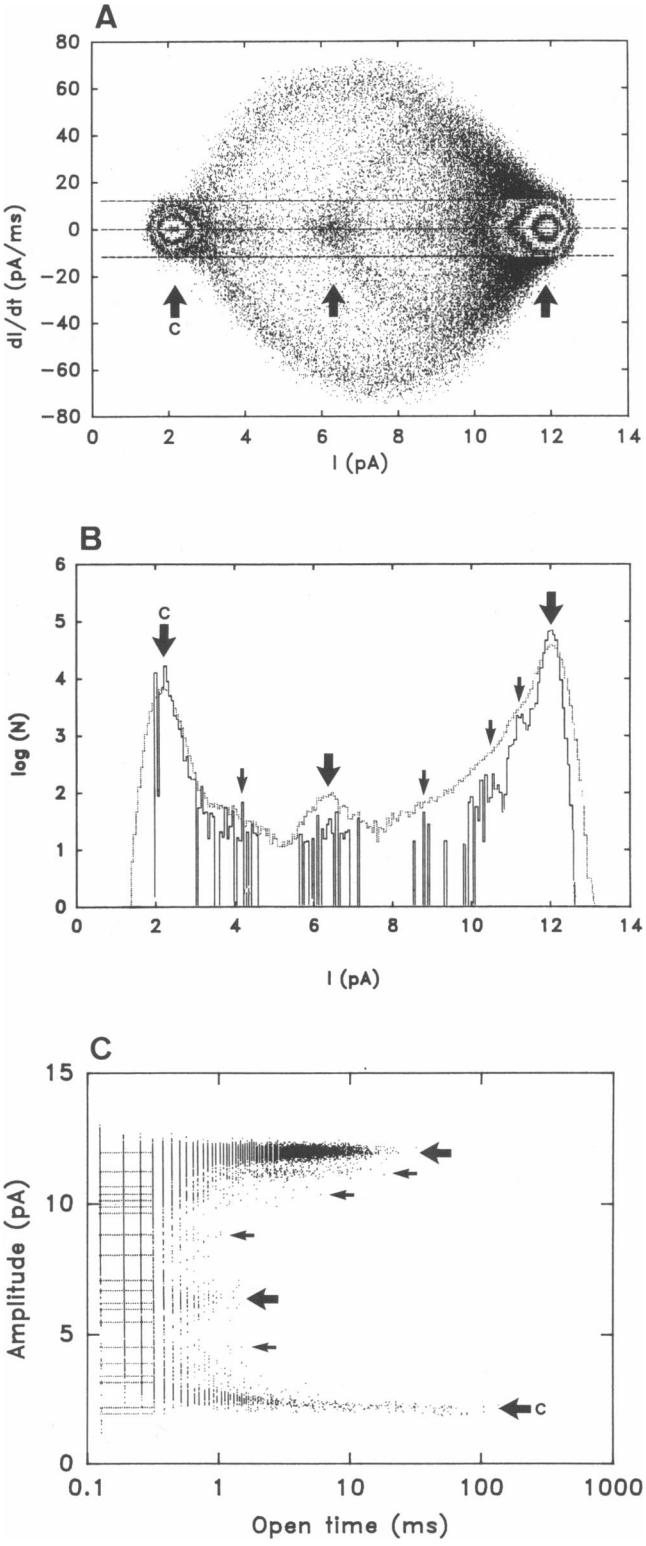

FIGURE 3 Results obtained for the K^+ channel in a drop-attached patch at a pipette p.d. of 100 mV (experiment 22989c). p.d. values and currents are pipette with respect to bath. (*A*) Rate-amplitude plot. The arrows indicate the closed level (labeled *C*), midstate, and mainstate. The upper and lower horizontal lines give the thresholds in dI/dt used to detect transitions. The contours at the two prominent nodes give an indication of the density of points. (*B*) Amplitude histograms. The dashed line is the distribution of all points not associated with a transition; the solid line gives the distribution of mean amplitudes weighted according to the duration. Large arrows are as in *A*; small arrows indicate other conductance states. (*C*) Amplitude versus duration obtained from the events list. The lines to the left of the data are the mode points from the mean amplitude distribution. Arrows are as in *B*.

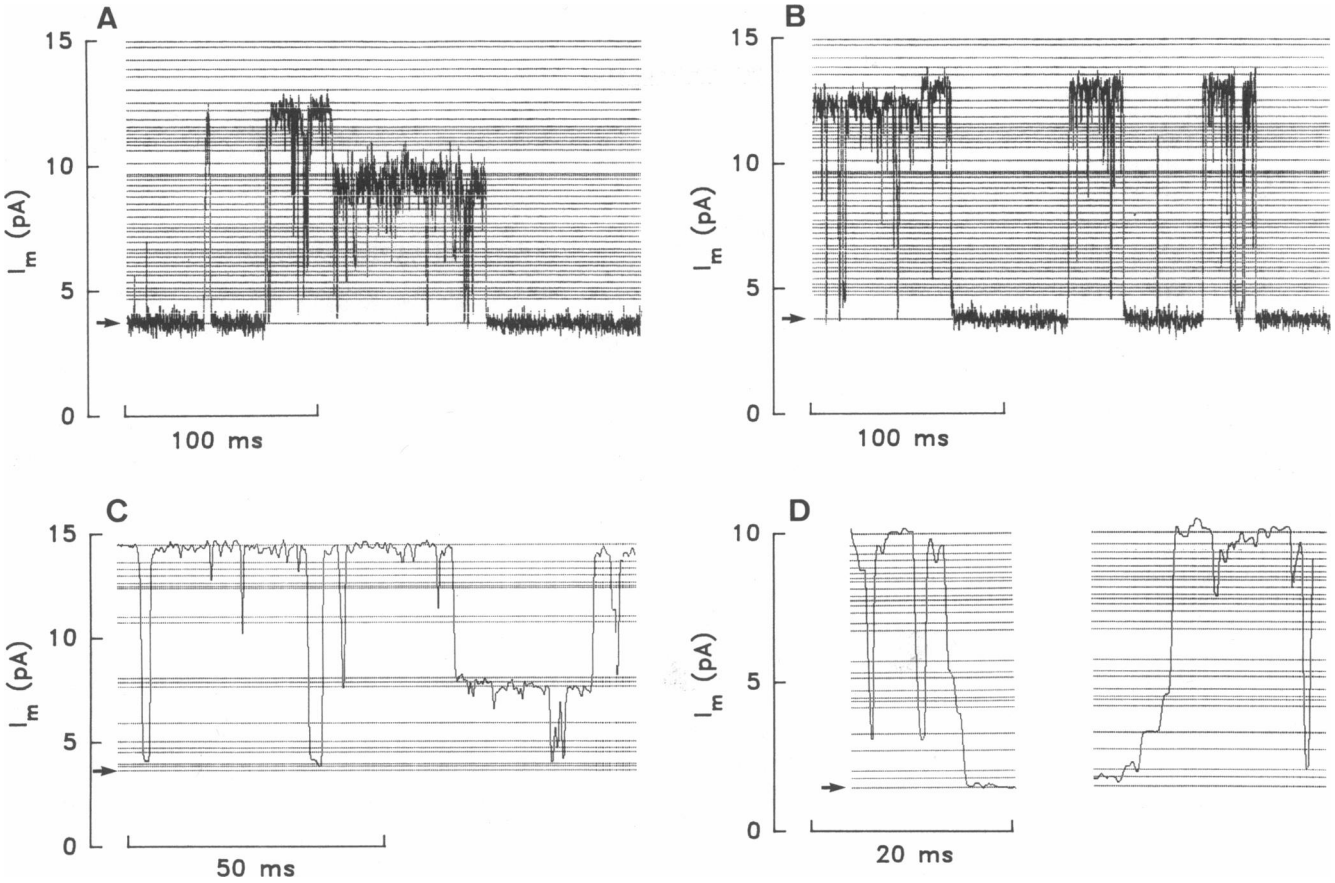

FIGURE 4 Single channel records of the K^+ channel from drop-attached patches showing examples of transitions between substates. In all examples p.d. values and currents are pipette with respect to bath. The horizontal lines on the figures are the mode points from the mean amplitude distribution. The horizontal arrows indicate the closed level. (*A* and *B*) Long duration substates observed in a patch held at 100 mV and 24°C (experiment 21391). (*C*) An unusually long midstate sojourn showing transitions between the midstate and closed level. Drop-attached patch at 100 mV and 24°C (experiment 22989c). Sampled at 5 kHz, filtered at 1 kHz. (*D*) Closing and opening through substates for a drop-attached patch, 100 mV, 10°C (experiment 101089a).

potential for Cl^-. To avoid ambiguities in the analysis, only patches without Cl^- channel activity were used.

Although the rate amplitude plots indicate that most transitions to the midstate occur from the mainstate (e.g., Fig. 3 *a* and Fig. 9), inspection of the raw data reveals that rare transitions can also occur between the midstate and closed state (Fig. 4, *c* and *d*). Also, if the channel closed from the midstate, it appeared to be able to then open directly to the mainstate (data not shown).

A characteristic better revealed by low temperature experiments was the existence of long lived conductance states around the fully open level. Duration/amplitude plots for a long record of channel activity for an inside-out patch (Fig. 5) show that these states could lead to some ambiguity in deciding where the fully open level is actually situated. Note that similar levels are not observed near the closed level, indicating that the small transitions are not due to the activity of another channel with a small conductance. The long lived substates also occurred in drop-attached patches at 24°C (Fig. 3, *b* and *c*; Fig. 4, *a* and *b*). These long lived conductances could not arise from the activity of more than one K^+ channel, each channel with slightly different conductances, because one channel would then have to open at exactly the same time as another closed.

2. Inside-out and outside-out patches

Inside-out and outside-out patches with low Ca^+ concentration at the cytoplasmic face showed substate behavior similar to drop-attached patches. This indicates that substate activity is not altered by patch excision (cf. Weik et al., 1989). The rate amplitude plot for an outside-out patch (Fig. 6) and amplitude-duration plot

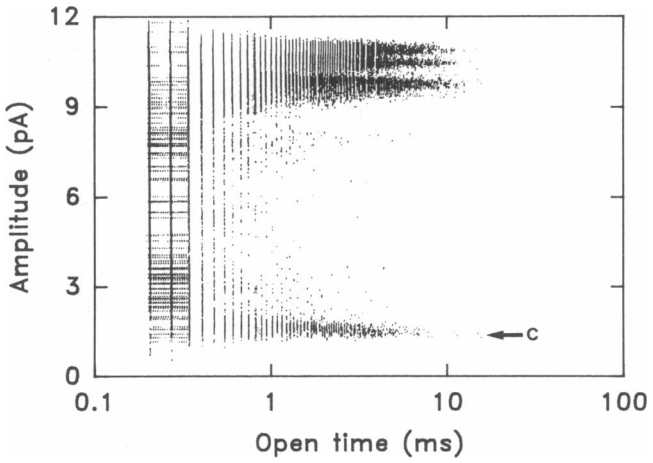

FIGURE 5 Amplitude-duration plot for data obtained from a K^+ channel in an inside-out patch held at 100 mV (pipette with respect to bath) and at 11°C (experiment 23390f2). Three segments of data, 26 s each, from a record totalling ~160 s have been superimposed to show more clearly the long duration current levels about the mainstate. The arrow indicates the closed state (labeled *C*). The horizontal lines to the left are mode values from the mean amplitude histogram. Bath solution (mol m^{-3}): 100 KCl, 2 EGTA, 5 HEPES, pH 7.2.

for an inside-out patch (Fig. 5) show that both the midstate and long duration upper levels occur in detached patches.

On some occasions inside-out patches were obtained with the cytoplasmic face of the membrane exposed to the standard bath solution containing 10 mol m^{-3} Ca^+. In three of four patches the substate behavior was opposite to the usual, with the channel occupying one of three low level conductance states for long periods (Fig. 7). Occasionally the channel would step up briefly to the normal fully open level.

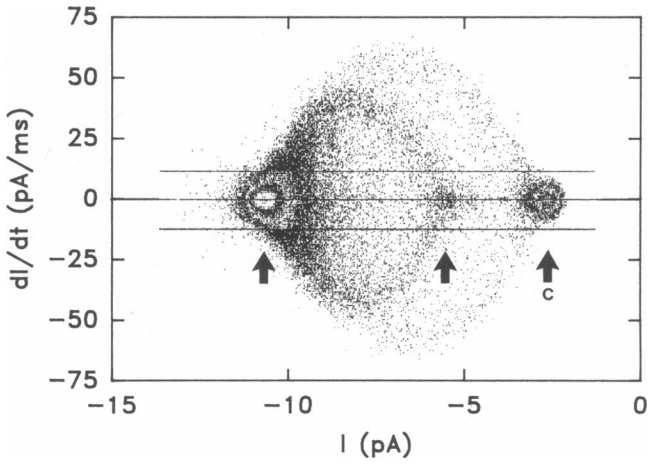

FIGURE 6 Results from a K^+ channel in an outside-out patch held at −100 mV (pipette with respect to bath) (experiment 131290e). For 5 s of record the rate-amplitude plot clearly shows the midstate with the predominant arc of transitions to and from the mainstate. The arrows indicate the closed level (labeled *C*), midstate, and mainstate. Pipette solution (mol m^{-3}): 90 Na Glutamate, 10 KCl, 2 EGTA, 10 HEPES, 15 KOH, pH 7.8.

3. Different concentrations of KCl

Currents through the K^+ channel were also examined with 200 and 500 mol m^{-3} KCl in the pipette solution for drop-attached patches. This was done to better resolve the individual substates, because the magnitude of the currents at positive pipette potentials is larger. From the amplitude histogram shown in Fig. 8, for 500 mol m^{-3} KCl and a pipette potential of 80 mV, it can be seen that at least six (possibly eight) conductance states can be identified (cf. Fig. 3).

4. Current-voltage curves

The rate/amplitude plots in Fig. 9 for one particular experiment at 11°C reveal a large number of transitions occurring to the midstate and serve to illustrate that the midstate current is not a constant proportion of the mainstate current at different p.d. Fig. 10 shows the current-voltage curves of the mainstate and midstate for

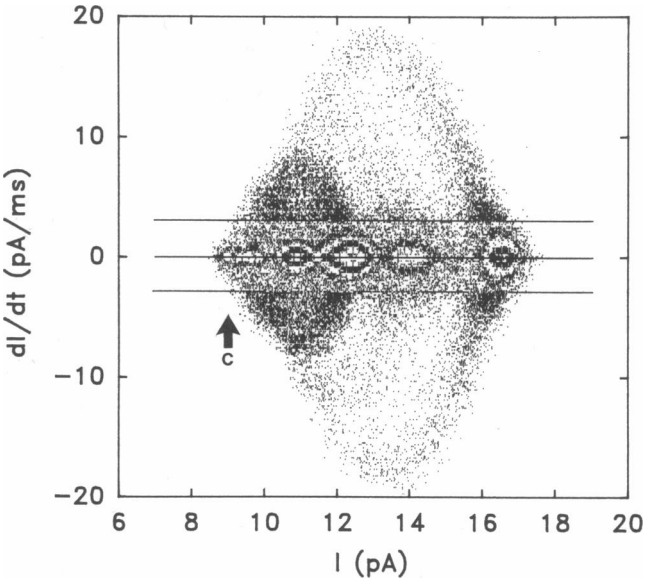

FIGURE 7 Rate-amplitude plot of the K^+ channel in an inside-out patch held at 77 mV (pipette with respect to bath) with 10 mol m^{-3} Ca^+ on both sides of the membrane (experiment 14391a). The channel appeared to reverse its normal behaviour by spending most of the time in middle-level substates and showing most transitions to the closed state (labeled *C*). Sampled at 5 kHz, filtered at 1 kHz.

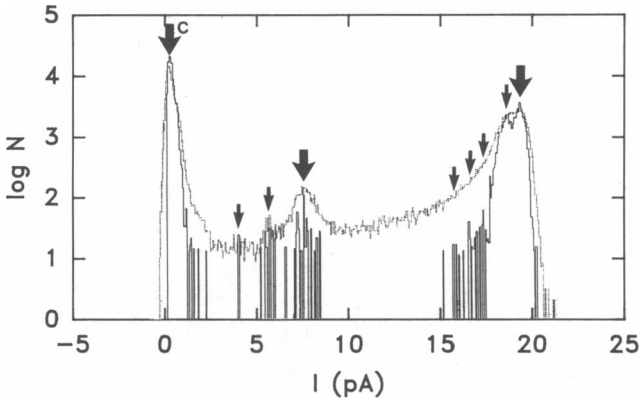

FIGURE 8 Amplitude histograms of the K^+ channel in a drop-attached patch with standard solution and 500 mol m^{-3} KCl in the pipette (experiment 3790h). For ~15 s of recording at 81 mV (pipette with respect to bath) several levels are discerned in the mean amplitude histograms (*arrows*). The large arrows indicate the closed level (labeled *C*), midstate, and mainstate.

a large range of membrane potentials across a drop-attached patch. It can be seen that the two curves have different shapes with the midstate curve showing substantial inward rectification. The I/V curves intersect at the same membrane p.d. as determined by cubic polynomials fitted to the data. This was also the case for different KCl concentrations in the pipette for drop-attached patches (Fig. 11, *a* and *b*).

IPROC and FETCHAN were also run on the set of data used to obtain the results in Fig. 10. FETCHAN was set with two thresholds to detect the current levels of the midstate and mainstate, and the calculated currents agreed with the TRAMP results. However, both IPROC and FETCHAN tended to underestimate the magnitude of inward currents for the mainstate. For example, at −172 mV the single channel estimate from IPROC and FECHAN/PSTAT was −13.77 and −13.59 pA respectively, while that obtained from TRAMP was −14.34 pA. With the amplitude threshold programs, multiple passes with different singles thresholds will produce more accurate results.

5. Kinetics

The durations of the mainstate and midstate displayed single exponential distributions (Fig. 12) indicating that each consists of only one kinetic state. The mean durations at 24°C for both states as determined by TRAMP were weakly dependent on membrane p.d. (Fig. 13), decreasing as membrane p.d. becomes more negative. This was observed in all experiments. At positive membrane p.d. the mean duration of the mainstate tended to decrease while that for the midstate continued to increase. The effect of low temperature on durations was variable between preparations but qualitatively appeared to increase durations of all states. These results will not be discussed here because more experiments are required in which channel currents are measured in the same patch and at different temperatures.

The fraction of the channel open-time spent in the midstate was less than 10% and decreased steeply with more negative p.d. values (Fig. 14). This was observed under a variety of conditions. In most experiments the number of transitions between the mainstate and midstate were greater than between the mainstate and closed state. This can be seen in Fig. 15 which shows an amplitude distribution of both positive and negative transitions. Fig. 15 also shows that the positive and negative transitions occurred at equal frequencies for all magnitudes (see superposition in the figure).

IPROC and FETCHAN give distributions of mainstate durations that are well fitted by a single exponential. The mean durations of the same set of data as analyzed by TRAMP are shown plotted versus membrane p.d. in Fig. 13. Both IPROC and FETCHAN yield similar durations for the mainstate which fit the parabolic voltage dependency described by Laver (1990), who also used IPROC for analysis of his data. The midstate durations can be determined using FETCHAN and these agree with those determined by TRAMP. At membrane p.d. more positive than ~−140 mV IPROC replaces transitions to the midstate with complete closures, presumably due to the fact that these pass the set threshold of 50% of the full current level. An example of this is shown in Fig. 16 for a membrane p.d. of −92 mV. For p.d. values more negative than ~−140 mV, the midstate current level moves closer to the mainstate and lies above the 50% threshold and is therefore combined with the mainstate. This has the effect of decreasing the estimated current amplitude of the mainstate.

DISCUSSION

It is clear from our data that conductance substates exist in the *Chara* tonoplast K^+ channel. The substate signature seems fairly robust in the sense that the same patterns were observed in inside-out, outside-out, and drop-attached patches as well as at different temperatures. The same is true for the animal Na^+ channel (Patlak, 1989) but not for the Ca^{2+}-activated K^+ channel from rat skeletal muscle which shows more substate activity after patch excision (Weik et al., 1989). Although the overall pattern of substates appears to be relatively stable we cannot discern the exact number of substates in the K^+ channel. There are two reasons

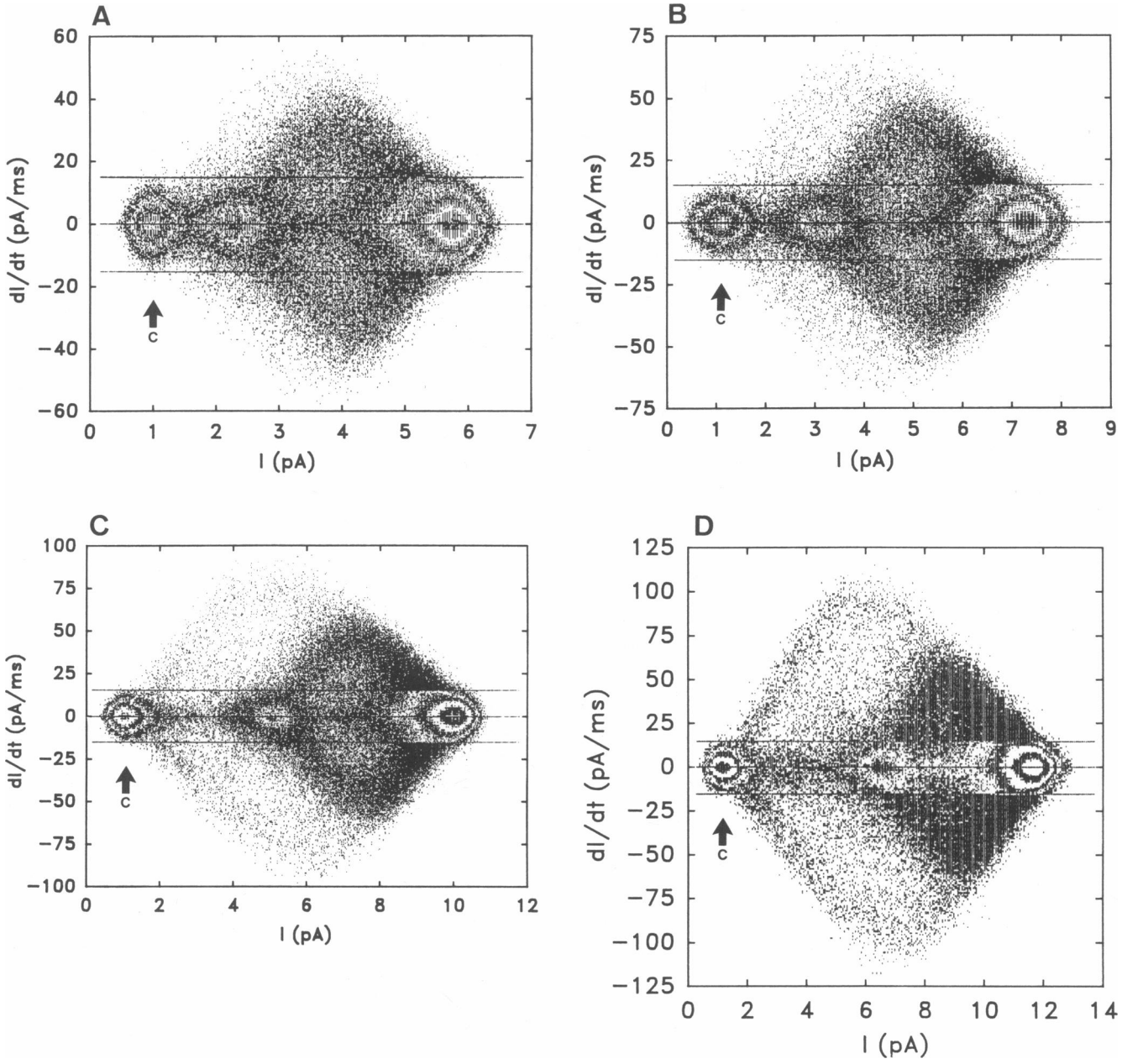

FIGURE 9 Rate amplitude plots of the K^+ channel in a drop-attached patch at 11°C and at different holding potentials (experiment 61089). p.d. values and currents are pipette with respect to bath. (*A*) 50 mV, (*B*) 70 mV, (*C*) 100 mV, (*D*) 120 mV. The arrows indicate the closed state (labeled *C*).

contributing to this uncertainty. First, there are long lived conductance levels near the mainstate whose number and activity is variable. Second, total amplitude histograms suggest that there may well be more conductance states that have not been resolved because of their short duration. At present we cannot tell whether the long tail on the amplitude histogram descending from the mainstate is due to unresolved transitions to the closed and midstate or due to many other substates. The mean amplitude histogram (Fig. 3 *b*) reveals some of these other substates within the tail of the total amplitude plot. It remains possible that there is a continuum of substates within the conductance range of the channel.

In animal systems it is becoming apparent that conductance substates may have physiological roles (Premku-

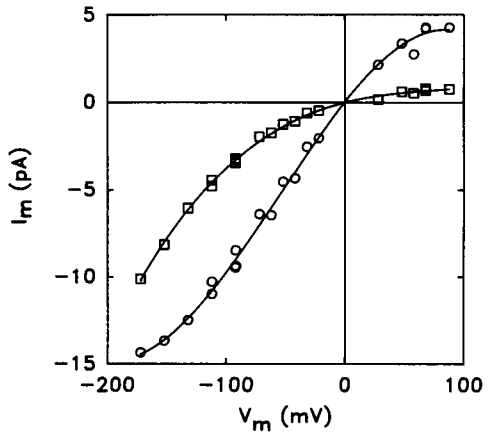

FIGURE 10 Current-voltage curve for the mainstate (○) and midstate (□) of the K^+ channel in a drop-attached patch (experiment 21391). p.d. values and currents have been corrected to give the normal convention (inside of drop with respect to bath). The lines are cubic polynomial fits.

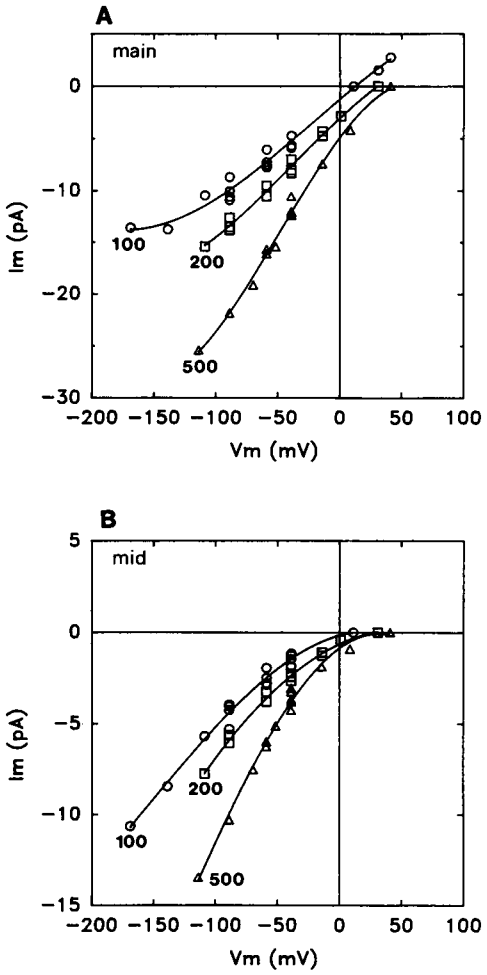

FIGURE 11 Current-voltage curves for the mainstate (*A*) and midstate (*B*) of the K^+ channel in drop-attached patches with different KCl concentrations (100, 200, 500 mol m^{-3}) in the standard pipette solution. Symbols on the voltage axis are at the reversal potentials. The midstate and mainstate had equal reversal potentials at the same KCl concentration.

mar et al., 1990). Variable conductance as well as gating gives another means of control of time averaged current through an ion channel. We have not found, with any certainty, any particular physiological circumstances that change the characteristics of the substate behavior of the K^+ channel in *Chara*. High concentrations of calcium on the cytoplasmic face of the tonoplast did modify the substate behavior in some cases. However, we are uncertain of the significance of this result because of the lack of consistent responses and the high calcium concentrations used (10 mM compared with physiological concentrations less than 1 μM). In the presence of reducing agents, a K^+ channel in the tonoplast of *Saccharomyces* becomes more sensitive to cytosolic calcium (Bertl and Slayman, 1990). It may be profitable to examine substate behavior in the *Chara* K^+ channel under similar conditions.

The substates in the K^+ channel in *Chara* are not always obvious for two reasons: (*a*) the long lived substates are very close to the mainstate conductance; (*b*) substates farther removed from the mainstate occur for a small fraction of the time that the channel is open, but can occur at a very high frequency. These two factors combined can lead to some false conclusions regarding both the conductance and kinetic behavior of the channel. For example, it could be wrongly concluded that the transitions to the midstate represent closures not fully resolved because of limited recording bandwidth. With IPROC analysis, transitions to substates are generally recorded as full closures. On the other hand, transitions to substates closer to the mainstate are counted as continuation of the mainstate event by both IPROC and FETCHAN. This results in longer mean durations recorded for the mainstate at negative membrane potentials by these two programs compared with those obtained from TRAMP. For TRAMP, any transition from the mainstate larger than the slope threshold terminates a particular event so that mean durations are assigned to individual detected levels. The duration between closed events (the "open-channel duration") is not obtained directly from TRAMP but could be obtained from the events lists. The open-channel duration is not reliably obtained from IPROC or FETCHAN because transitions to the midstate are counted as closures. IPROC and FETCHAN will both indicate the presence of substates, for example, the total amplitude histograms

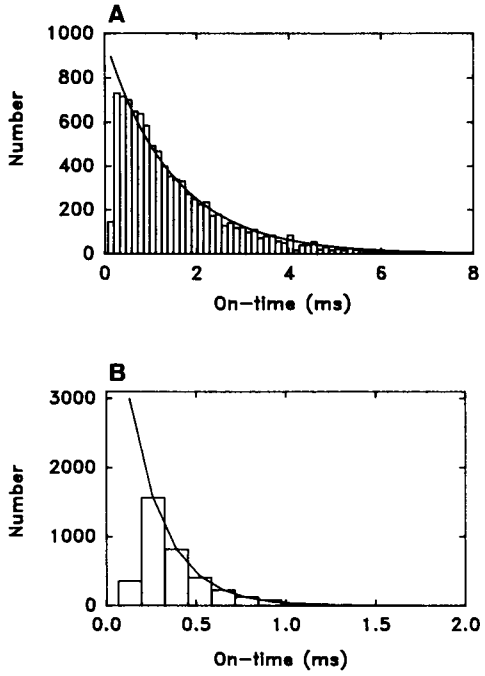

FIGURE 12 Distributions of the durations of the mainstate (*A*) and midstate (*B*) for the K^+ channel in a drop-attached patch, 100 mV pipette p.d. and 11°C (experiment 61089). The distributions are fitted by a single exponential with time constants of 1.3 ms (mainstate) and 0.23 ms (midstate).

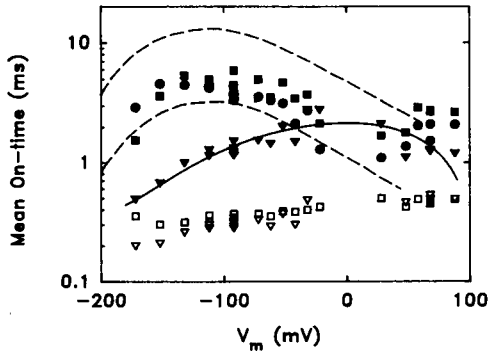

FIGURE 13 Durations of the mainstate (*solid symbols*) and midstate (*open symbols*) of the K^+ channel as a function of membrane p.d. (experiment 21391) using different analysis programs. The IPROC (●) and FETCHAN (■) analysis gives mainstate durations significantly longer than those obtained from TRAMP (▼) for membrane p.d. values less than ~ −50 mV. They lie within the 90% confidence limits determined by Laver (1990). The line fitted to the TRAMP data is a cubic polynomial. The substate durations determined by TRAMP (▽) and FETCHAN (□) are in reasonable agreement.

from both programs and flicker-pulse average from IPROC.

Both IPROC and FETCHAN use 50% thresholds to detect transitions to new levels. Since the midstate changes its conductance relative to the mainstate as a function of membrane p.d., IPROC and FETCHAN will count transitions to the midstate as closures at some membrane p.d., and as fluctuations in the mainstate level at other p.d. values. As a result, the "open-channel durations," as measured by IPROC and FETCHAN, will be inaccurate and the true variation with membrane p.d. will be masked.

It was on the basis of IPROC analysis that Laver and Walker (1987), Laver, Fairly and Walker (1989), and Laver (1990) proposed that there were two distinct closed states into which the *Chara* tonoplast K^+ channel could enter. They showed that the mean open duration had a maximum at ~ −120 mV, a result confirmed by us using FETCHAN and IPROC. To obtain this peak in duration there would need to be at least two ways in which the mainstate (O_1) could be terminated to two closed states (C_1 and C_2). The rate constants for the transitions would have apparent opposite voltage dependencies. In Laver et al. (1989), their basic scheme, ignoring their other closed states, would be:

$$C_1 \rightleftharpoons O_1 \rightleftharpoons C_2. \quad (1)$$

Since transitions from the mainstate to the midstate can be more frequent than transitions to the closed state (particularly at more positive membrane p.d. values), then it might be possible to account for the results of Laver et al. by transitions to the midstate (O_2) rather than complete closures, i.e.:

$$C \rightleftharpoons O_1 \rightleftharpoons O_2 \rightleftharpoons C. \quad (2)$$

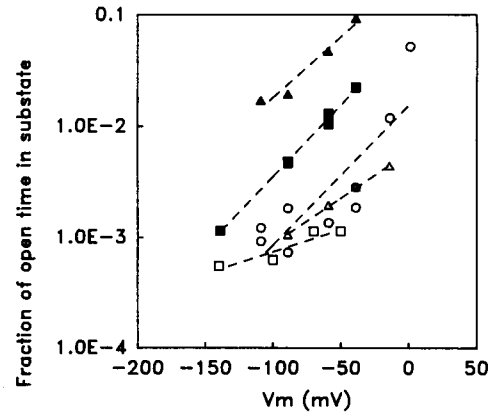

FIGURE 14 Fraction of the open channel time which is spent in the midstate as a function of membrane p.d. and under a variety of experimental conditions. (▲) Drop-attached, 11°C. (■) Drop-attached, 24°C. (□) Inside-out, 11°C. (○) Drop-attached, 200 mol m^{-3} KCl, 14°C. (△) Drop-attached, 200 mol m^{-3} KCl, 24°C.

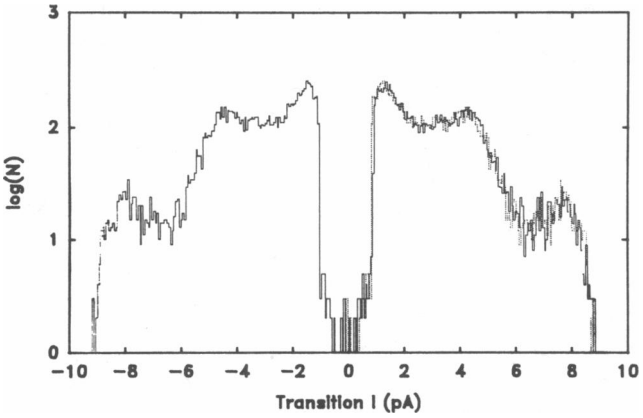

FIGURE 15 Distribution of transition amplitudes for the K^+ channel in a drop-attached patch at 100 mV pipette p.d. and 11°C (experiment 61089). The negative going transitions (*left*) have been superimposed on the positive transitions (*right*).

IPROC analysis would lead to scheme 1 rather than scheme 2 because IPROC counts midstate transitions as closures. As argued above, the apparent voltage dependency of open-durations as determined by IPROC can arise from the change in midstate current relative to the mainstate current as a function of membrane p.d. This is superimposed upon a real reduction in mainstate duration and midstate frequency with decreasing membrane p.d. Since the transitions $O_2 \leftrightarrow C$ are much less frequent than $O_1 \leftrightarrow O_2$, we can calculate the rate constant to a first approximation for $O_2 \rightarrow O_1$ from the mean durations of O_2. At −100 mV this was 3,371 s^{-1} (SD = 384 s^{-1}, $n = 6$). This mean rate is similar to 3,960 s^{-1} (SD = 1314 s^{-1}, $n = 5$) obtained by Laver and Walker (1987) for closed state C_2 to O_1 (scheme 1). Given that IPROC can treat transitions to the midstate as closures it is possible that C_2 identified by Laver and Walker (1987) represents the midstate.

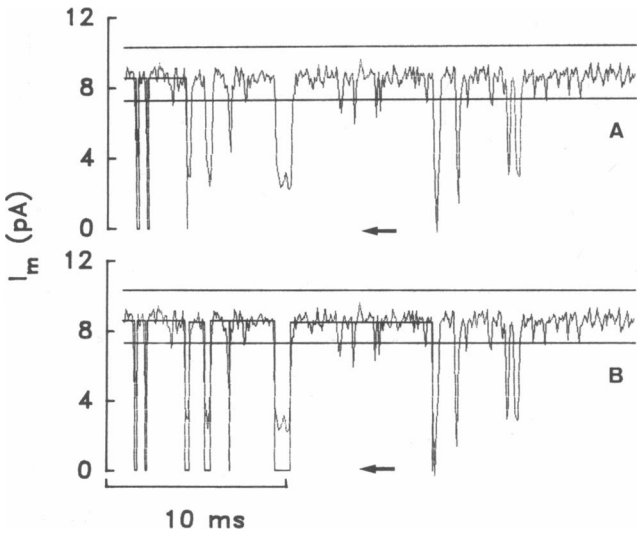

FIGURE 16 Portion of a record of single channel current through the K^+ channel showing the midstate before (*A*) and after (*B*) analysis with IPROC (experiment 21391). The idealized current trace superimposed on the raw data by IPROC shows closures where in reality transitions to the midstate have occurred. The arrow indicates the closed level.

A number of channels exhibiting subconductances have been modeled as a group of cochannels coordinated in their gating behavior in some way, e.g., by the presence of a main gate which can close all cochannels simultaneously (Hunter and Giebisch, 1987). In our case the mainstate is unlikely to be made up of a number of identical cochannels, because the conductance levels we observe are not evenly spaced. Similar results have been observed for other channels (Fox, 1987) including the animal Na^+ channel (Patlak, 1988), a K^+ channel in the plasma membrane of *Acetabularia* (Bertl et al., 1988), and a K^+ in the tonoplast of barley (Kolb et al., 1987). However, as noted above there may be other as yet unresolved substates in the *Chara* K^+ channel so the possibility exists that there may be many small units of equal conductance making up the full conductance. Each of these units would have to have quite different probabilities of becoming uncoupled from the main gating mechanism to lead to the observed substate signature. One difficulty with this model as applied to the *Chara* K^+ channel is that the ratio of a substate's conductance to the mainstate can vary as a function of membrane p.d., at least for the prominent midstate conductance. It is possible that we may not be dealing with the same "midstate" at each p.d., but instead a range of subconductances where the probability of visiting a particular "midstate" varies with p.d. One way of resolving this improbable suggestion would be to apply fast voltage ramps similar to the method used to define substates of a Cl^- channel in *Amaranthus* plasma membrane (Terry et al., 1991). The construction of single channel current-voltage surfaces from ramps (Sansom and Mellor, 1990) would also give the current-voltage curves for the other substates.

The reduced conductance and strong inward rectification of the midstate could arise from an increase in overall energy barrier height with a shift in the peak of this barrier towards the cytoplasmic side of the pore. In terms of the electrodiffusion model of Laver and Walker (1987), it could be explained by a constriction of the cytoplasmic vestibule (or the equivalent in terms of charge) resulting in lowered permeability of this aqueous convergence region. This variable constriction model has been referred to as the "stenosis model" (Hill et al.,

1990). Substates would result from transient and favored increases in heights of energy barriers or depths of energy wells that reduce permeation within the pore. The constrictions to permeation may arise from: (*a*) the main gating mechanism, or mechanisms (see Laver, 1990) making partial closures; (*b*) alteration of the ionic environment within or near the pore perhaps via H^+ binding (Prod'hom et al., 1987); (*c*) changes in pore diameter or dipole interactions due to transient conformational changes induced by thermal vibrations or by binding of permeant ions (Pietrobon et al., 1988) or other ions (e.g., Ca^{2+} or H^+).

Inspection of the data shows that transitions occur between the midstate and the closed state and that after a closure from the midstate the channel can open directly to the mainstate. This indicates that the midstate transitions fit to cyclical schemes rather than to a series scheme. A cyclic reaction incorporating the midstate does not cycle preferentially in any direction (see Fig. 15), indicating that it is at equilibrium (Colquhoun and Hawkes, 1983). This is not the case for the double-barrelled Cl^- channel from *Torpedo* electroplax (Richard and Miller, 1990).

CONCLUSION

The K^+ channel from *Chara* tonoplast displays a complex multiconductance behavior. If the substates are ignored, the kinetic behavior of the channel will not be correctly determined. It is possible that these separate conductance states may be regulated by an as yet unknown factor or factors. In particular, cytosolic calcium concentrations may be important together with other modifying conditions (e.g., pH, K^+ concentration, redox potential). Further investigations may yet reveal the biophysical significance of multiple conductance levels, which careful observation reveals to be common to nearly all ion channels.

The experimental observations of Nele Findlay and Guy Sander are gratefully appreciated. We thank Alan Walker for drawing our attention to median filters, and Derek Laver for stimulating discussions on models of the K^+ channel.

This work was supported by the Australian Research Council.

Received for publication 28 June 1991 and in final form 22 October 1991.

REFERENCES

Auerbach, A., and F. Sachs. 1983. Flickering of a nicotinic ion channel to a subconductance state. *Biophys. J.* 42:1–10.

Auerbach, A., and F. Sachs. 1984. Single-channel currents from acetylcholine receptors in embryonic chick muscle. Kinetic and conductance properties of gaps within bursts. *Biophys. J.* 45:187–198.

Bertl, A., H. G. Klieber, and D. Gradmann. 1988. Slow kinetics of a potassium channel in *Acetabularia*. *J. Membr. Biol.* 102:141–152.

Bertl, A., and C. L. Slayman. 1990. Cation-selective channels in the vacuolar membrane of *Saccharomyces:* dependence on calcium, redox state, and voltage. *Proc. Natl. Acad. Sci. USA.* 87:7824–7828.

Chung, S.-H., J. B. Moore, L. Xia, L. S. Premkumar, and P. W. Gage. 1990. Characterization of single channel currents using digital signal processing techniques based on hidden markov models. *Phil. Trans. R. Soc. Lond. B.* 329:265–285.

Colquhoun, D., and A. G. Hawkes. 1983. The principles of the stochastic interpretation of ion-channel mechanisms. *In* Single-Channel Recording. B. Sakmann and E. Neher, editors. Plenum Press, New York. 135–175.

Colquhoun, D., and F. J. Sigworth. 1983. Fitting and statistical analysis of single-channel records. *In* Single-Channel Recording. B. Sakmann and E. Neher, editors. Plenum Press, New York. 191–263.

Fox, J. A. 1987. Ion channel subconductance states. *J. Membr. Biol.* 97:1–8.

Geletyuk, V. I., and V. N. Kazachenko. 1985. Single Cl^- channels in molluscan neurones: multiplicity of the conductance states. *J. Membr. Biol.* 86:9–15.

Hamill, O. P., and B. Sakmann. 1981. Multiple conductance states of single acetylcholine receptor channels in embryonic muscle cells. *Nature (Lond.).* 294:462–464.

Hill, J. A., R. Coronado, and H. C. Strauss. 1990. Open-channel subconductance state of K^+ channel from cardiac sarcoplasmic reticulum. *Am. J. Physiol.* 258:159–164.

Hunter, M., and G. Giebisch. 1987. Multi-barrelled K channels in renal tubules. *Nature (Lond.).* 327:522–524.

Jackson, M. B. 1988. Dependence of acetylcholine receptor channel kinetics on agonist concentration in cultured mouse muscle fibres. *J. Physiol.* 397:555–583.

Justusson, B. I. 1981. Median filtering: statistical properties. *In* Topics in Applied Physics. Vol. 43. Two-Dimensional Digital Signal Processing II. Transforms and Median Filters. T. S. Huang, editor. Springer-Verlag, Berlin. 161–196.

Kazachenko, V. N., and V. I. Geletyuk. 1984. The potential-dependent K^+ channel in molluscan neurones is organized in a cluster of elementary channels. *Biochim. Biophys. Acta.* 773:132–142.

Kolb, H.-A., K. Kohler, and E. Martinoia. 1987. Single potassium channels in membranes of isolated mesophyll barley vacuoles. *J. Membr. Biol.* 95:163–169.

Laver, D. R., and N. A. Walker. 1987. Steady-state voltage-dependent gating and conduction kinetics of single K^+ channels in the membrane of cytoplasmic drops of *Chara australis*. *J. Membr. Biol.* 100:31–42.

Laver, D. R., K. A. Fairley, and N. A. Walker. 1989. Ion permeation in a K^+ channel in *Chara australis:* direct evidence for diffusion limitation of ion flow in a maxi-K channel. *J. Membr. Biol.* 108:153–164.

Laver, D. R. 1990. Coupling of K^+-gating and permeation with Ca^{2+} block in the Ca^{2+}-activated K^+ channel in *Chara australis*. *J. Membr. Biol.* 118:55–67.

Lucchesi, K., and E. Moczydlowski. 1990. Subconductance behaviour in a maxi Ca^{2+}-activated K^+ channel induced by dendrotoxin-1. *Neuron.* 2:141–148.

Lühring, H. 1986. Recording of single K^+ channels in the membrane of cytoplasmic drop of *Chara australis*. *Protoplasma.* 133:19–28.

Miller, C. 1982. Open-state substructure of single chloride channels from *Torpedo* electroplax. *Phil. Trans. R. Soc. Lond. B.* 299:401–411.

Mistry, D. K., and J. J. Hablitz. 1990. Activation of subconductance states by γ-aminobutyric acid and its analogs in chick cerebral neurons. *Pfluegers Archiv.* 416:454–461.

Patlak, J. B. 1989. Sodium channel subconductance levels measured with a new variance-mean analysis. *J. Gen. Physiol.* 92:413–430.

Pietrobon, D., B. Prod'hom, and P. Hess. 1988. Conformational changes associated with ion permeation in L-type calcium channels. *Nature (Lond.).* 333:373–376.

Premkumar, L. S., P. W. Gage, and S.-H. Chung. 1990. Coupled potassium channels induced by arachidonic acid in cultured neurons. *Proc. R. Soc. Lond. B.* 242:17–22.

Prod'hom, B., Pietrobon, D. and Hess, P. 1987. Direct measurement of proton transfer rates to a group controlling the dihydropyridine-sensitive Ca^{2+} channel. *Nature (Lond.).* 329:243–246.

Richard, E. A., and C. Miller. 1990. Steady-state coupling of ion-channel conformations to a transmembrane ion gradient. *Science (Wash. DC).* 247:1208–1210.

Sachs, F., J. Neil, and N. Barkakati. 1982. The automated analysis of data from single ionic channels. *Pfluegers Arch.* 395:331–340.

Sansom, M. S. P., and I. R. Mellor. 1990. Analysis of the gating of single ion channels using current-voltage surfaces. *J. Theor. Biol.* 144:213–223.

Sawyer, D. B., R. E. Koeppe, and O. S. Anderson. 1989. Induction of conductance heterogeneity in gramicidin channels. *Biochemistry.* 28:6571–6583.

Sigworth, F. J., D. W. Urry, and K. U. Prasad. 1987. Open channel noise. III. High-resolution recordings show rapid current fluctuations in gramicidin A and four chemical analogues. *Biophys. J.* 52:1055–1064.

Strecker, G. J., and M. B. Jackson. 1989. Curare binding and the curare-induced subconductance state of the acetylcholine receptor channel. *Biophys. J.* 56:795–806.

Terry, B. R., Tyerman, S. D. and Findlay, G. P. 1991. Ion channels in the plasma membrane of Amaranthus protoplasts: one cation and one anion channel dominate the conductance. *J. Membr. Biol.* Vol. 121:223-236.

Trautman, A. 1982. Curare can open and block ionic channels associated with cholinergic receptors. *Nature (Lond.).* 298:272–275.

Tyan, S. G. 1981. Median filtering: deterministic properties. *In* Topics in Applied Physics. Vol. 43. Two-Dimensional Digital Signal Processing. II. Transforms and Median Filters. T. S. Huang, editor. Springer-Verlag, Berlin. 197–217.

Tyerman, S. D., G. P. Findlay, and B. R. Terry. 1989. Behaviour of K^+ and Cl^- channels in the cytoplasmic drop membrane of *Chara corallina* using a transient detection method of analysing single-channel recordings. *In* Plant Membrane Transport. J. Dainty, M. I. De Michelis, E. Marre, and Rasi-Caldogno, editors. Elsevier, Amsterdam. 173–178.

Tyerman, S. D., and G. P. Findlay. 1989. Current-voltage curves of single Cl^- channels which coexist with two types of K^+ channel in the tonoplast of *Chara corallina*. *J. Exp. Bot.* 40:105–117.

Vivaudou, M. B., J. J. Singer, and J. V. Walsh. 1986. An automated technique for analysis of current transitions in multilevel single-channel recordings. *Pfluegers Arch.* 407:355–364.

Weik, R., U. Lönnendonker, and B. Neumcke. 1989. Low-conductance states of K^+ channels in adult mouse skeletal muscle. *Biochim. Biophys. Acta.* 983:127–134.